Performance Considerations for Protected Wideband Satcom

Thomas C. Royster and James Streitman
MIT Lincoln Laboratory
Lexington, MA 02420

***Abstract*—There is increased interest in using transponded payloads to provide jam-resistant links to users. In the type of system we consider, multiple user terminals transmit to a satellite using a coordinated frequency hopping waveform, and the received signals are relayed to a ground processing "hub" terminal for baseband processing. In this paper, expressions for computing end-to-end signal-to-noise ratios for such systems are presented, and some example results are provided. In particular, modeling of effects such as signal suppression, intermodulation noise, and gain setting is discussed. By considering each component of the end-to-end link performance separately, the factors limiting performance are more apparent, enabling the system designer to identify which improvements would have the greatest impact.**

I. Introduction

As the demand for protected MILSATCOM increases, approaches for augmenting the current protected MILSATCOM portfolio are of great interest. For purposes of this paper, by "protected" we mean having the ability to employ the allocated spectrum (whether it be limited by system allocation, allocated beam or beams, satellite configuration, etc.) for bandwidth spreading and achieving most or all of the theoretical jam-resistance corresponding to that spreading bandwidth. One approach to achieve some level of jam-resistant communication for users is to utilize existing or future transponded satellites as part of a broader protected system design. For example, [1] describes a current effort to assess the performance and affordability trades of several protected MILSATCOM design approaches.

Relative to satellites that perform waveform processing onboard the satellite, transponded satellites are typically associated with link performance losses and increased latency. In this paper, the issue of link performance losses is considered in detail. Expressions for transponded link performance that account for nonlinear effects and interference are presented, and the implementation considerations associated with each are discussed. In addition to the analytical expressions, corresponding simulation results are also provided for comparison.

II. System Description

A basic illustration of the system under consideration is provided in Figure 1. A transponded satellite has at least one user beam, each of which provides coverage to one or more users. The satellite also has one or more hub beams, each of which provides coverage to a waveform processing hub. Thus, a hub-spoke configuration is employed. The combination of satellite and hub is referred to as the space segment. Functionally, this setup is equivalent to a satellite with on-board processing, in that for an on-board processing satellite, the set of space segment functions is housed completely within the satellite.

This work is sponsored by the Air Force under Air Force Contract #FA8721-05-C-0002. Opinions, interpretations, conclusions, and recommendations are those of the author and are not necessarily endorsed by the United States Government.

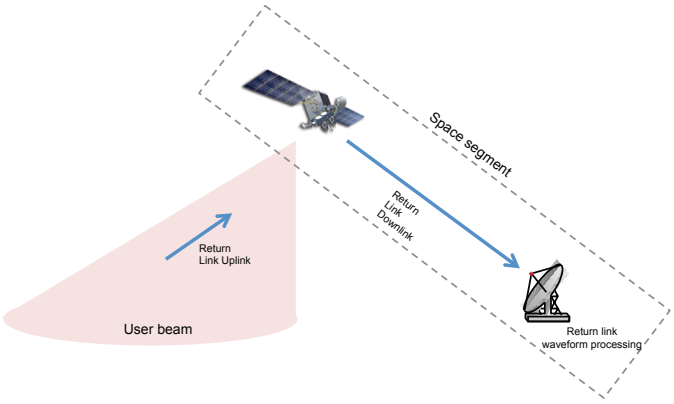

Fig. 1. Example illustration of a hub-spoke transponder system configuration.

A user return link consists of an uplink from a user to the satellite along with a downlink from the satellite to a hub. A user forward link consists of an uplink from a hub to the satellite along with a downlink from the satellite to a user. In this paper, we are primarily interested in characterizing the performance of the return link.

III. Key Performance Components

In this section, expressions are presented for computing a user's end-to-end ratio of power to noise density, P_r/N_0, in a pure transponder system. We consider a scenario in which N terminals transmitting on the uplink to a satellite using orthogonal channels, and the aggregate received multichannel signal is relayed by the satellite to a ground processing hub.

In a transponder system servicing N simultaneous FDMA users, the fraction of downlink power corresponding to user i's signal is given by

$$P_{d,i} = \frac{S_i}{\sum_{j=1}^{N} S_j + N_u W_S + J} \alpha P, \tag{1}$$

where S_j is the received uplink power from the jth transmitter, N_u is the uplink noise density, W_S is the spread spectrum bandwidth, and J is the jammer power. This equation is also valid when an orthogonal frequency hopping waveform is used,

978-1-5090-0073-9/15/$31.00 ©2015 IEEE

since at any instant of time the aggregate received uplink spectrum corresponding to such a waveform is equivalent to that of a non-hopping FDM waveform.

The expression in (1) quantifies what is typically referred to as *power sharing*. *Power robbing* is a term commonly used to describe situations in which a large value of jammer power J or uplink noise N_u causes $P_{d,i}$ to have a value significantly less than what would result in the absence of noise or jamming. The parameter α is the signal suppression parameter. Signal suppression is a well-known phenomenon that can occur when multiple signals simultaneously pass through a nonlinear function, such as a hard-limiting or clipping amplifier, and there is a dominant signal. Generally, there is no suppression if the device is kept perfectly linear (e.g., with ideal automatic gain control). Otherwise, it is well-known that a 1 dB suppression is obtained when a dominant AWGN signal is present in a nonlinear device, and up to a 6 dB suppression is obtained when the dominant signal is continuous-wave (CW). More information on signal suppression can be found in [2], [3], and [4].

The density of the noise and interference present at the receiver is upper bounded by the expression

$$N_0 \leq N_d + \left[(1-\beta) \frac{N_u W_S + J}{\sum_{j=1}^{N} S_j + N_u W_S + J} + \beta \right] \frac{P}{W_S}, \quad (2)$$

where N_d is the density of the downlink noise, and the parameter β models the additional noise incurred due to nonlinearities in the payload. In (2), it is assumed that the spreading bandwidth W_S is equal to the transponder bandwidth W_T.

Combining (1) and (2), a bound on the end-to-end P_r/N_0 is obtained:

$$\begin{aligned} (P_r/N_0)_i \quad \geq \quad & \\ & \left(\frac{N_u}{\alpha S_i} + \frac{J/W_S}{\alpha S_i} \right. \\ & + \frac{\beta(\sum_{j=1}^{N} S_j + N_u W_S + J)/W_S}{\alpha S_i} \\ & + \left. \frac{N_d}{P} \frac{\sum_{j=1}^{N} S_j + N_u W_S + J}{\alpha S_i} \right)^{-1}. \end{aligned} \quad (3)$$

Note that in this paper we will represent the components as noise-to-signal ratios where convenient, but discussion of the components are typically in terms of their inverses, the signal-to-noise ratios. It is clear from (3) that there are four primary contributors to the end-to-end P_r/N_0. First is the uplink signal-to-noise ratio, as expected. The remaining three components of the end-to-end P_r/N_0 are discussed in the following subsections.

A. Jammer Contribution to Uplink Noise

The second term in (3) captures the contribution of the jammer signal to the ith user's received signal's noise floor. The formulation that appears in (3) is based on the assumption that the total jammer power J is uniformly spread across the entire spreading bandwidth W_S and that the effects are equivalent to additive white Gaussian noise. The framework of equation (3) does not preclude modeling of other power distributions within the spreading bandwidth. For time intervals in which no jammer signal is directly present in the ith user's channel, this term can be set to zero. Of course, during these time intervals it is possible that jammer signals could be present in other frequency channels in the transponder, but the corresponding impacts to user i's performance are modeled in other terms of (3).

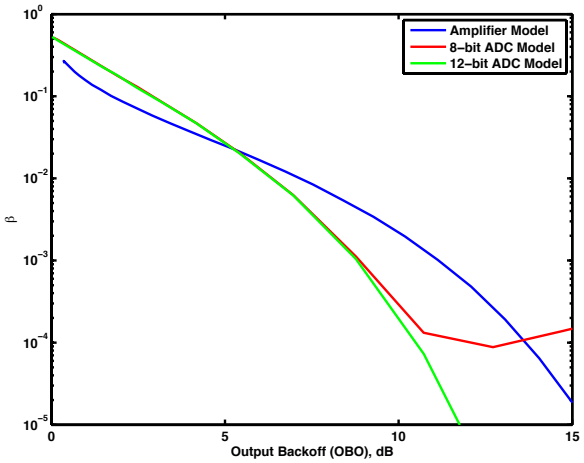

Fig. 2. Values of β for an amplifier model and two ADC models.

B. Intermodulation Noise

The third term of (3) accounts for noise induced by payload nonlinearities. Some methods employ noise power ratio (NPR) (e.g., [5]) rather than β, where NPR is the ratio of all uplink signal, noise, and interference power to intermodulation power. NPR is related to β by

$$\beta = (\mathrm{NPR} - 1)^{-1}. \quad (4)$$

In the third term of (3), the term in parenthesis is the total amount of uplink signal power captured by the transponder. The resulting noise density is the total received power scaled by the parameter β and assumed to be spread across the transponder bandwidth.

Ultimately, the value of β depends on the linearity of the operating region of the nonlinear device, so each is a function of the output back off (OBO), where OBO is defined as the ratio of the average output power to the maximum output power of the device. Examples are provided in Figure 2 for an analog amplifier model as well as an 8-bit and a 12-bit analog-to-digital converter, in which β is given as a function of OBO. The amplifier curve is derived from the model used for all remaining amplifier results in this document. The analog-to-digital converter (ADC) models, which represent digitizing transponders, are ideal uniform, balanced quantizers.

For values of OBO near 0 dB, the two ADC models result in larger (worse) values of β than does the amplifier model. In the Figure, the 8-bit ADC model exhibits a leveling off of the value of β and then an increase as OBO exceeds approximately 11 dB, which is due to increased quantization noise of not using some of the ADC's dynamic range when the OBO is too large.

C. Downlink Noise

The last term of (3) accounts for the net effect of noise at the downlink receiver and the downlink power allocated to transmission of the ith user's signal. The ratio P/N_d is the ratio of transmitted downlink power to the downlink noise density. Specifically, P represents the total amount of power from the satellite after accounting for OBO. The remainder of the expression provides the fraction of received uplink power due to the ith user's signal.

This component of the end-to-end P_r/N_0 accounts for power sharing. The design choices that influence this component include hub link strength (satellite antenna, satellite amplifier, hub antenna), number of users, and OBO. In fact, while increasing OBO generally reduces intermodulation noise, the effects of downlink noise may be increased due to reduced downlink transmit power. (In a later section, such tradeoffs are considered further.) The jammer component of this expression accounts for the total amount of jammer power present in the processing bandwidth, regardless of whether any of the jammer signal is present in the channel containing user i's signal.

IV. Simulation Description

A system with 125 MHz of spreading bandwidth is considered. 125 return link users are employing an orthogonal frequency-hopping (FH) waveform using QPSK with root-raised cosine (RRC) pulse shaping. Each user is allocated 1 MHz of bandwidth, the location of which changes periodically due to the FH waveform. The remaining details of the FH waveform are unimportant for purposes of this paper, as the aggregate P_r/N_0 values we wish to compute are for instantaneous snapshots in time. For noise and interference that is constant across frequency and time, the P_r/N_0 values can be used to determine specific data rates and modes that could be closed for a specified waveform. If the link has variations in frequency or time, then the waveform performance must be computed based on a series of instantaneous P_r/N_0 values as appropriate.

Each transmitter generates a known random sequence of PSK symbols, performs pulse shaping with an RRC filter. All the users' signals are combined into a multiple carrier signal. The uplink channel introduces AGWN noise at a specified noise power level. The jamming signal is then added, which for the results in this paper is either wideband noise or hard-limited wideband noise.

The simulation model determines an end to end bit error rate of a modulated waveform in a variety of scenarios. The input signal to the transponder model consists of K adjacent carriers of such signals. This signal represents the aggregate uplink transmissions of K terminals.

Depending on the simulation parameters, the transponder then performs gain control, hard or soft limiting, ADC effects, power measurements and amplification using the amplifier model. The downlink channel then applies AWGN, and the total signal is processed in the receiver. Specifically, for each carrier, matched filter detection is used to determine the received data sequence. This received sequence is compared against the known transmitted data sequence to determine the number of bit errors in each carrier. The number of bit errors across all carriers is averaged, and an equivalent signal-to-noise ratio is computed.

V. Implementation Considerations

In assessing the end-to-end return link performance, we can consider the constituent terms of (3). In many cases, the end-to-end performance is limited by one or two of the constituent terms and the other terms do not have a significant influence. All else equal, the performance of a transponder-based system is upper bounded by an on-board processed (OBP) system. The last term of (3) is not present for such a system since a downlink is not involved in the return link. As such, the expression for P_r/N_0 for a processed system is given by

$$(P_r/N_0)_{i,\mathrm{OBP}} \geq \left(\frac{N_u}{\alpha S_i} + \frac{J/W_S}{\alpha S_i} + \frac{\beta(\sum_{j=1}^{N} S_j + N_u W_S + J)/W_S}{\alpha S_i} \right)^{-1}. \quad (5)$$

The intermodulation term of (5) is dependent on the implementation of the OBP receiver's front end. Two potential approaches are for the ADC to capture the entire spreading bandwidth (e.g., [6]) or to capture only the channel bandwidth. The channel bandwidth is typically much smaller than the spreading bandwidth, so available ADCs for this approach generally have larger dynamic ranges than ADCs used to capture the entire spreading bandwidth. With a larger dynamic range, there is a larger range of operating points having very low values of β (e.g., see Figure 2), in which case the intermodulation component may be ignored in many cases.

In this paper, results are presented in terms of E_s/N_0, which is the ratio of the energy per channel bit to the density of the thermal noise. For uncoded QPSK, there are two channel bits per modulation symbol. If R is the number of channel bits transmitted per second, then E_s/N_0 and P_r/N_0 are related by $P_r/N_0 = RE_s/N_0$. In the remaining figures, the "component signal-to-noise ratios (SNRs)" are plotted alongside the aggregate E_s/N_0 values. Each component SNR is the ratio of the energy per channel bit to the density of the component's noise, assuming a Gaussian distribution.

In Figure 3, the uplink component and the jammer component are plotted in blue and red, respectively. The intermodulation component is assumed to be negligible for the

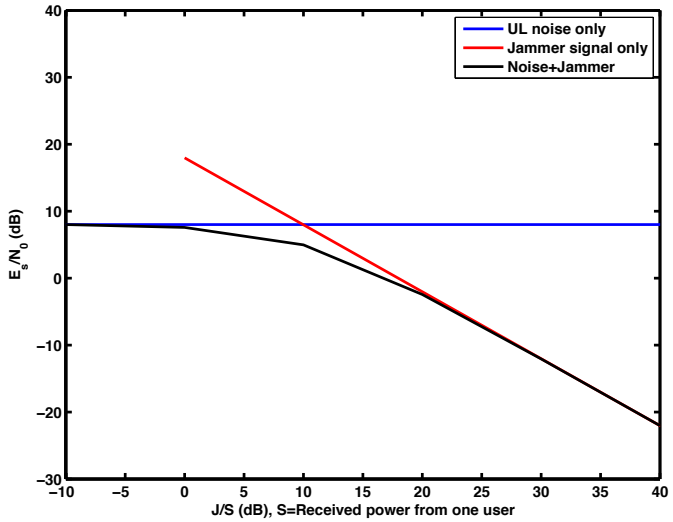

Fig. 3. Constituent SNRs for an on-board processed system.

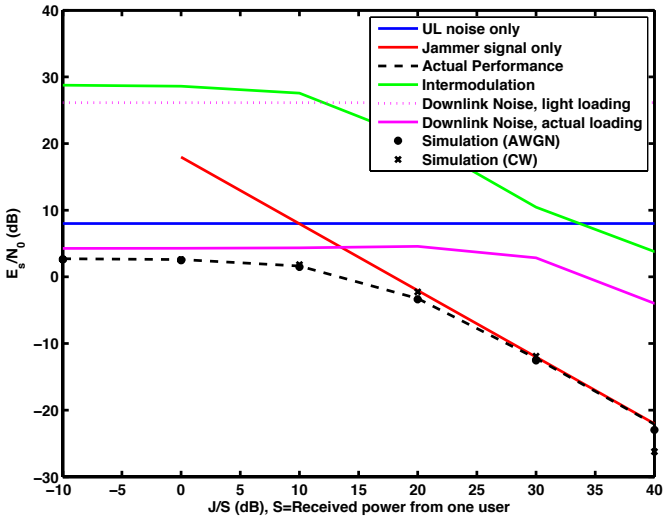

Fig. 4. Constituent SNRs: 1.58 m hub, 125 users, AGC off, 11.6 dB OBO (benign).

moment. The resulting aggregate E_s/N_0, represented by the black line, has three regions. For low values of J/S, uplink noise is dominant. For high values of J/S, the jammer noise is dominant. In these two regions, the aggregate E_s/N_0 matches the SNR of the dominant component. The third region is where the two components are similar in magnitude, such that the aggregate E_s/N_0 is significantly influenced by both components and is thus lower than both (for example, when both constituent SNRs are equal, the aggregate E_s/N_0 is 3 dB less than the constituent value).

Thus, if the goal for a transponder-based system is to have equivalent performance to an on-board processed system, then the former must be designed such that the downlink SNR does not significantly influence the aggregate E_s/N_0. As mentioned previously, there are also some dependencies between the downlink SNR and the intermodulation SNR that must be considered. On the other hand, the performance target of a transponder-based system may be relaxed relative to an equivalent OBP system, in which case the effects of downlink and intermodulation SNRs may be allowed to influence the aggregate E_s/N_0.

VI. Performance Results

In this section, example design considerations for transponder systems are considered along with the resulting aggregate and constituent SNRs.

For example, Figure 4 includes the constituent SNRs as a function of the ratio of jammer power to user power for a hub employing a 20 GHz downlink frequency, a 1 m satellite antenna for hub coverage, and a 1.58 m hub antenna. A fixed satellite gain is employed, such that there is an 11.6 dB OBO when 125 users are present. The four solid lines correspond to the four terms on the right-hand-side of (3). The dashed line represents the resulting aggregate SNR. For low values of J/S, performance is limited by the downlink SNR. For larger values of J/S, however, the performance is limited by the direct jammer effects. Note that for this example, the intermodulation noise does not influence the end-to-end SNR, since other noise sources dominate performance across the entire range of J/S.

Simulation results are represented as discrete points. For a wideband AWGN interferer, the performance exactly matches that of the analytical expressions except for $J/S = 40$ dB, where the effects of signal suppression are observed (the α parameter was assumed equal to unity for all the curves generated from analytical expressions in this paper). For a wideband CW interferer, larger values of signal suppression are observed, as expected.

Analytical results for the same configuration as in Figure 4 are shown in Figure 5, with the exception that the use of automatic gain control (AGC) is assumed along with a fixed OBO of 9 dB. Thus, the system remains linear regardless of input power level. If an AGC is employed at the input to the nonlinear device, the input signal power seen by the device is kept constant regardless of actual fluctuations in received power. In general, the output power of the device, and thus the OBO, also remains constant as a result. In contrast, if a fixed gain setting is used instead, as the aggregate incoming signal to the satellite fluctuates in power, those fluctuations are also present at the input to the device. Depending on the device's operating point, the fixed gain setting implies that the OBO varies as the input power varies.

For larger values of J/S, the downlink SNR has a minor influence on the aggregate SNR since the output power is decreased relative to that of the system of Figure 4. Note that the intermodulation SNR does not decrease in this case since the AGC ensures the payload nonlinearities do not increase as the input power increases. For this setup, however, limiting the nonlinear effects does not have any major impact on the aggregate performance. Rather, improving the downlink SNR would be more worthwhile. In addition, the fixed-gain approach may also be preferred at the system level because its operation

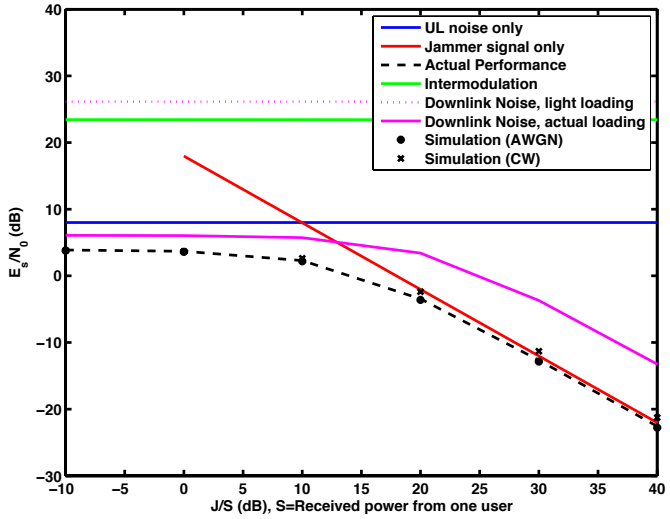

Fig. 5. Constituent SNRs: 1.58 m hub, 125 users, AGC on, 9 dB OBO.

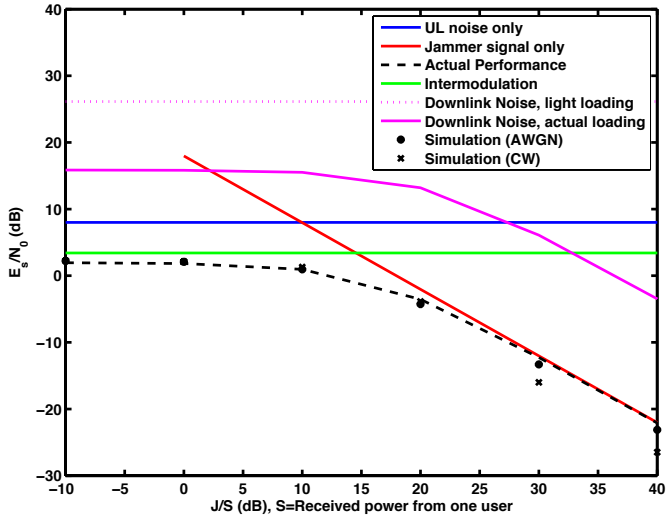

Fig. 6. Constituent SNRs: 1.58 m hub, 125 users, hard-limited (0 dB OBO).

has no potential vulnerabilities (e.g., algorithms, loops).

One method by which the downlink SNR could be improved is by further decreasing the OBO. The performance results of Figure 6 are for the extreme case of operating at 0 dB OBO, which is equivalent to hard-limiting. The downlink SNR is seen to improve so much that it no longer limits performance over the entire range of J/S. The consequence of such low OBO is that the nonlinear payload effects are very large; in fact, the intermodulation SNR is now what limits the performance at low values of J/S. Furthermore, the signal suppression results observed in the simulation results now happen for smaller values of J/S, since the payload is always operating in a heavily nonlinear mode.

From a performance standpoint, a better method for improving downlink SNR is to increase the size of the hub antenna while maintaining some OBO in the payload. With this approach, the downlink SNR improves, but the intermodulation

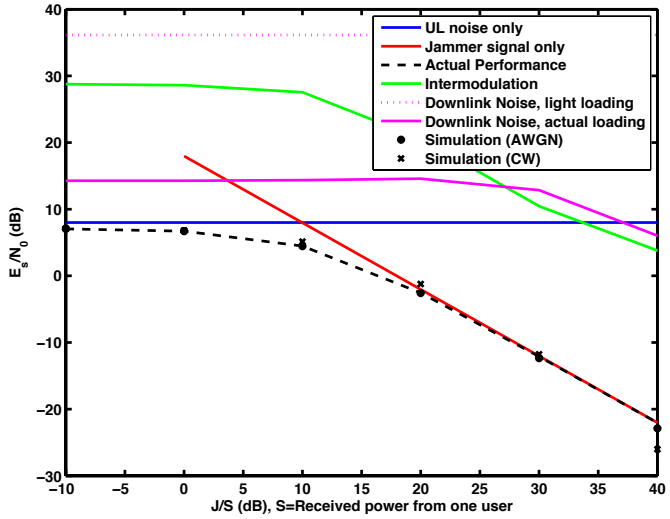

Fig. 7. Constituent SNRs: 5 m hub, 125 users, AGC off, 11.6 dB OBO (benign).

SNR remains high. Figure 7 provides an illustration of the performance obtained with a 5 m hub antenna. The aggregate SNR essentially matches that of the aggregate SNR of an OBP system; in fact, at low values of J/S, the aggregate SNR is within 1 dB of what would be obtained with an OBP system. To reduce the gap, a larger hub antenna could be employed, or perhaps a better tradeoff between intermodulation SNR and downlink SNR could be found by adjusting the OBO.

VII. Mesh Considerations

As highlighted in the previous section, the size of the receive hub antenna plays a significant role in obtaining performance that approaches that of OBP. For this reason, hub-spoke configurations are generally the preferred approach in obtaining the best possible jamming resistance from a transponded satellite. On the other hand, other aspects of OBP systems are desirable, such as not having to rely on a hub for communications and reduced communications latency. To obtain these benefits, transponded mesh configurations are required.

In a sense, the same design considerations of the previous section also apply for mesh configurations. If the user population consists of terminals with large antennas, then achieving good link performance with a mesh configuration is feasible because a good downlink SNR can be maintained. On the other hand, if some users have relatively small antennas, then the aggregate performance may be dominated by the downlink SNR across the range of J/S values. An example of this phenomenon is provided in Figure 8. Even for large values of J/S, the effects due to power robbing on the downlink are more significant than the actual interference from the jammer.

VIII. Conclusion

Performance modeling of transponded systems has been presented in terms of the constituent SNRs in order to clearly

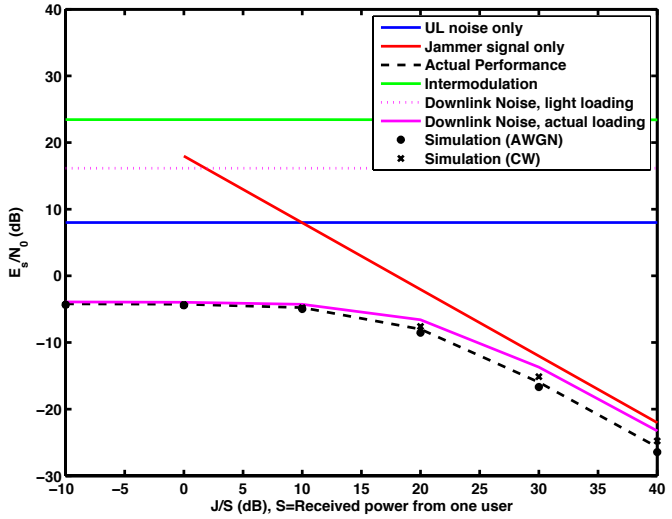

Fig. 8. Constituent SNRs: 0.5 m hub, 125 users, AGC on, 9 dB OBO.

illustrate which aspects of the system design influence performance under which set of circumstances. Except when the transponder is purposefully operated in a heavily nonlinear mode (e.g., to support disadvantaged receivers), effects such as intermodulation noise and signal suppression do not drive performance, as the direct jammer effects tend to be the limiting factor. This is consistent with the analysis in [7]. Rather, the primary design goal is to ensure that the downlink SNR per channel does not drive overall performance. Towards this end, improving the quality of the hub link by increasing the satellite antenna size, hub antenna size, or satellite amplifier size on this link (or some combination) is preferred over significantly reducing amplifier OBO.

We have illustrated tradeoffs involved in transponder link design, from which it can be shown how to achieve performance approaching that of OBP satellites. In the broader system design, however, other considerations such as latency, spectrum availability, satellite resource efficiency, hub vulnerabilities, and number of coverages, for example, must be considered in the overall tradespace. Transponder-based systems generally fare worse than OBP systems in these areas. For applications that can tolerate the broader implications of employing transponder-based systems, however, achieving reasonable levels of jamming resistance is possible.

IX. Acknowledgment

The authors would like to thank Tom Seay for many valuable insights and for providing the framework of equations (1) and (2).

References

[1] M. Glaser, et al., "Protected MILSATCOM design for affordability risk reduction (DFARR)," *IEEE Military Communications Conference*, pp. 998–1001, November 2013.

[2] J. L. Sevy, "The effect of limiting a biphase or quadriphase signal plus interference," *IEEE Transactions on Aerospace and Electronic Systems*, vol. AES-5, no. 3, pp. 387–395, May 1969.

[3] P. D. Shaft, "Limiting of several signals and its effect on communication system performance," *IEEE Transactions on Communication Technology*, vol. COM-13, no. 4, pp. 504–512, December 1965.

[4] C. R. Cahn, "Calculation of intermodulation due to amplitude limiting of multiple carriers," *IEEE Transactions on Communication Technology*, pp. 743–745, December 1969.

[5] M. Lyubarev, et al., "Transponded architecture considerations in protected MILSATCOM," *IEEE Military Communications Conference*, pp. 1020–1025, November 2013.

[6] F. J. Block, "Performance of wideband digital receivers in jamming," *IEEE Military Communications Conference*, October 2006.

[7] E. B. Felstead and R. J. Keightley, "Robustness capabilities of transponded commercial satellite communications," *IEEE Military Communications Conference*, vol. 2, pp. 783–787, November 1995.